Sensorless Based Gravity Torque Estimation and Friction Compensation for Surgical Robotic System

Branesh M. Pillai, Dileep Sivaraman, Songpol Ongwattanakul, and Jackrit Suthakorn
Center for Biomedical and Robotics Technology (BART LAB),
Faculty of Engineering, Mahidol University, Thailand.

2022 IEEE 9th International Conference on e-Learning in Industrial Electronics (ICELIE) | 978-1-6654-8990-4/22/$31.00 ©2022 IEEE | DOI: 10.1109/ICELIE55228.2022.9969429

***Abstract*—This article intends to provide content that is both basic and elementary, but at the same time discusses how solving difficult challenges when estimating the actual force in real-time teleoperation using a small-size DC motor as the end effector/ gripper of the surgical robot. The end-effector of the surgical robot, where the surgical tools have been attached, requires high-end precision. Most commercial surgical robotic systems calculate the real-time force by using traditional force sensors which encounters hindrance like lack of expected response (advance control), limited bandwidth, and requirement of force for its own operation. The paper introduces a Disturbance observer (DOB) based Reaction Torque observer (RTOB) as the sensor for the real-time gravity torque sensing in biomedical applications, with a focus on surgical robots. In order to enable both professional engineers and students with a limited understanding of control to use the article, mathematical complications are kept to a minimum.**

***Index Terms*—DC motor parameter estimation, Disturbance observer, Bilateral control, Robotic surgery**

I. Introduction

Robot-assisted surgery will continue to accept and incorporate developments in a variety of main areas in the foreseeable future. It allows physicians to perform many forms of complex procedures with greater precision, versatility, and control than traditional techniques. As an advancement, surgical robot for teleoperation has been widely researched and developed. During Teleoperation procedures, as the surgeon is separated from the patient, he experiences a lack of direct palpation, tactile sensation, poor visibility, poor hand-eye coordination, inadequate depth details, and no proper force feedback from touching the organs and movement limitations [12]. Most of the prevalent teleoperation systems incorporates bilateral control systems (master and slave robots). In conventional bilateral control, much research has paid attention to developing control architectures and implementing force/torque sensors to detect external force. However, it is inappropriate to attach any electric or magnetic sensor for measuring force on a surgical robot instrument because the surgical robot instrument should be manufactured in small size and overcome safety problems caused by using electric or magnetic sensors in the human body [14].

A servo motor and its driver serve as the actuator, while a force/torque sensor and its controller measure force data from the physician and the patient, and a data acquisition card converts analog to digital–digital to analog. Encoder emulation is used to obtain position data. To get the appropriate reactions, DC servomotors employed in control applications should use precise control methods. In such applications, controller parameters must be fine-tuned to achieve the desired system response [8]. The physical parameters of the systems determine when controller parameters are tuned. As a result, it is critical to identify the precise physical properties of systems [11]. Estimating and compensating for DC motor friction is a challenging task that has been attempted by numerous researchers [4, 11, 13]. Nevertheless, there are some non-linearities that exist in DC motors, such as gravitational torque, which have to be compensated for precise motion.

The traditional force/torque sensors used in surgical robots are supposed to be positioned at different places which include actuator, gripper surface, or in an appropriate site and their range of force sensation will be restricted to the places where they are installed. Some inherited properties of these force sensors are responsible for causing errors in the output, e.g. the physical force sensor tends to add inertia or mass to the system, which will not be considered by the sensor during the estimation of reaction force. Additionally, they have narrow bandwidth and hence the measured force is significantly dull. Therefore, it is clear that the force sensors are not suitable with applications that demand high precisions like robotic surgery.

Taking into considerations the impediments imposed by the application requirements, Murakami et al proposed a force control method known as reaction torque/force observer (RTOB) [3]. The method of force control is based on disturbance observer (DOB), which is a common method to estimate and compensate the disturbance force. A reaction torque observer (RTOB/RFOB) system excludes system uncertainties such as friction from the disturbance input to estimate the reaction torque/force. This reaction torque/force forms a basis for feedback in a force control system without the use of any force sensors. Considering the implementation of robots in medical applications, which demands an appropriate force control method, the DOB-based RTOB lends a unique attribute of being sensorless without compromising the performance.

In this paper, the authors devise a method for designing and executing a system model to find out the disturbances and their effects on environment parameters [7, 3]. The material in this article is presented in a manner that gradually increases the complexity of the system, beginning with the fundamental DC motor control model, gravity torque compensation model,

The research has been funded by the Reinventing University System through Mahidol University, Thailand, (IO 864102063000).
*Corresponding author : jackrit.sut@mahidol.ac.th

Disturbance Observer model, and concluding with the bilateral control system towards the simulation. Using a DOB and RTOB a sensorless-based approach is incorporated into this paper. The nominal and the actual values of motor torque constant and motor inertia are made equal. Inertia and external torque are compensated by fine-tuning the system model appropriately [9]. Later a friction subsystem model is introduced based on the calculations of the friction parameter estimation. Except for gravity, the system has adjusted for all disturbances through friction compensation [10]. According to this system model, design is accomplished in Simulink. A disturbance of a particular kind is provided as input to the system. Later through fine-tuning, the same disturbance is obtained as the output from the DOB. The RTOB output obtained is zero, which implies the disturbances except gravity have been fully corrected. By executing this system in real-time, the output obtained in the RTOB is the gravity torque. Thus, gravity torque is estimated. The DC motor model is investigated in this research, and then a sensorless torque-sensing model is created utilizing the DOB and RTOB. The DC motor nonlinear parameters such as change of inertia, friction, and gravity values are estimated through mathematical modeling. The validation of estimated parameters in a bilateral system is executed.

II. MATERIALS AND METHODS

A. DC Motor Model

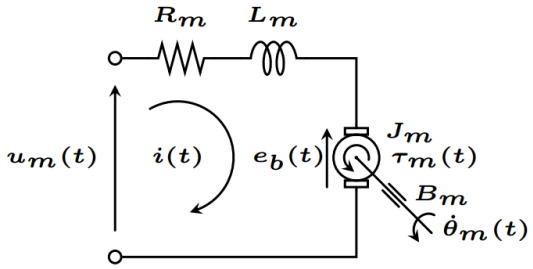

Fig. 1. DC motor

The equation of electric motor is [5]

$$u_m(t) = R_m {i_a}^{ref}(t) + L_m \frac{d{i_a}^{ref}(t)}{dt} + e_b + \tau_f(t) \quad (1)$$

where $u_m(t)$ is the input voltage, ${i_a}^{ref}(t)$ the reference current, $e_b(t)$ the counter-electromotive force, R_m the terminal resistance and Lm the robot inductance. The mechanical equation of the motor is [5]

$$\tau_m(t) = J_m \ddot{\theta}_m(t) + \tau_l(t) + \tau_f(t) \quad (2)$$

where $m(t)$ represents the motor torque, $\ddot{\theta}(t)$ the angular acceleration of the motor, J_m the rotor inertia, $\tau_l(t)$ the load torque from the motor axis and $\tau_f(t)$ the friction torque which considers different friction components such as the damping one amongst others. As a result, only the damping viscous torque will be considered [5].

$$\tau_m(t) = J_m \ddot{\theta}_m(t) + B_m \dot{\theta}_m(t) + \tau_l(t) \quad (3)$$

The angular motor velocity is $\dot{\theta}_m(t)$, the damping viscous torque is $B_m \dot{\theta}_m(t)$, and the damping viscous constant is B_m. A DC motor typically satisfies the electro-mechanical coupling equations:

$$e_b(t) = K_e \dot{\theta}_m(t) \quad (4)$$

$$\tau_m(t) = K_t i(t) \quad (5)$$

where K_e and K_t are motor constants, back-EMF constant and torque constant, respectively. When measured in the same unit system, $K_e = K_t$. Let t_e and t_m be the electric and mechanical time constants, respectively:

$$t_e = \frac{L_m}{R_m} \quad (6)$$

$$t_e = \frac{R_m + J_m}{R_m B_m + K_e K_t} \quad (7)$$

The DC motor equations can be simplified by considering that a DC motor's electric constant is usually much smaller than its mechanical constant, that is, $t_e \ll t_m$ [5]. This can be interpreted as eliminating the contribution of inductance L_m in the electric equation. As a result, equation (1) can be represented as:

$$u_m(t) = R_m {i_a}^{ref}(t) + K_e \dot{\theta}_m(t) \quad (8)$$

From the equations (3), (5), and (8)

$$u_m(t) = \frac{R_m J_m}{K_t} \ddot{\theta}_m(t) + (\frac{R_m B_m}{K_t} + k_b) \dot{\theta}_m(t) + \frac{R_m}{K_t} \tau_l(t) \quad (9)$$

A simplified equation of a DC motor for the non loading conditions can be written as:

$$\frac{K_t}{R_m} u_m(t) = J_m \ddot{\theta}_m(t) + (B_m + \frac{K_e k_t}{R_m}) \dot{\theta}_m(t) + \tau_l(t) \quad (10)$$

B. Gravity torque compensation model

When a load with gearbox of reduction factor $r \in (0; 1]$ and efficiency $\eta \in (0; 1]$ to attach the motor axis. Then, the angular velocity $\dot{\theta}_L(t)$ and load torque $\tau_L(t)$ at the gearbox output will be related to $\dot{\theta}_m(t)$ and $\tau_l(t)$ in the motor axis respectively:

$$\dot{\theta}_L(t) = r \dot{\theta}_m(t) \quad (11)$$

$$\tau_L(t) = \frac{\eta}{r} \tau_l(t) \quad (12)$$

The Euler-Lagrange equation can be used to find the dynamic equation. The Lagrangian L is defined as $L = K - V$, where K denotes the kinetic energy and V denotes the potential energy of the rigid body that rotates around axis z of the inertial reference system S_0 is given by

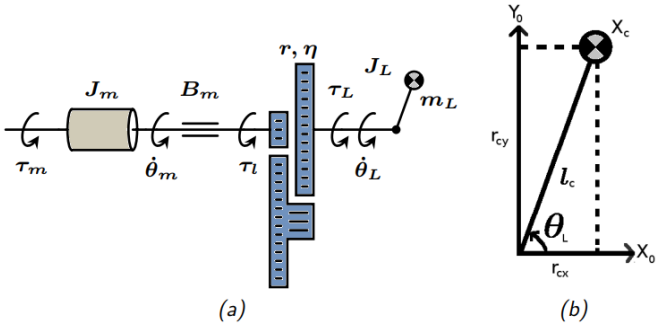

Fig. 2. (a) Side view and (b) frontal view of the axis, gearbox and DC motor load.

$$\tau_L(t) = \frac{d}{dt}(\frac{\partial L}{\partial \dot{\theta_L}}) - \frac{\partial L}{\partial \theta_L} \tag{13}$$

where $\tau_L(t)$ is the load torque. In the Cartesian coordinates of the center of mass in the system S_0 for a 1 DOF mechanism,

$$X_c = l_c \begin{bmatrix} cos\theta_L(t) \\ sin\theta_L(t) \\ 0 \end{bmatrix}$$

So the linear velocity of the center of mass v_c is obtained from X_c and the angular velocity $\tilde{\omega} = R_z\omega$, (where R_z is the rotation matrix between the S_0 and S_c reference systems) can be obtained from the derivative of the elemental rotation matrix around axis z.

$$v_c = \dot{X}_c = l_c\dot{\theta}_L \begin{bmatrix} -sin\theta_L(t) \\ cos\theta_L(t) \\ 0 \end{bmatrix}$$

$$\tilde{\omega} = \dot{\theta}_L(t)\vec{k} \begin{bmatrix} 0 \\ 0 \\ 1 \end{bmatrix}$$

$$r_{cy} = l_c sin\theta_L(t) \tag{14}$$

$$\tilde{\omega}^T I_c \tilde{\omega} = I_{zz}\dot{\theta}_L^2(t) \tag{15}$$

$$v_c{}^T v_c = l_c^2\dot{\theta}_L^2(t) \tag{16}$$

Since the kinetic energy

$$K = \frac{1}{2}mv_c^T v_c + \frac{1}{2}\tilde{\omega}^T I_c\tilde{\omega} \tag{17}$$

and potential energy

$$V = mgr_{cy} \tag{18}$$

Where $m = m_s + m_L$, and m_s represent mass of shaft and m_L represent mass of load. Equation (13) can solve from the equations of K, V, $\tilde{\omega}$, v_c, and r_cy,

$$\tau_L(t) = J_L\ddot{\theta}_L(t) + mgl_c cos\theta_L(t) \tag{19}$$

where $J_L = I_{zz} + ml_c^2$, r_{cy} is the y coordinate of the center of mass position, g is the acceleration due to gravity on earth, and I_c is the constant inertia tensor around the center of mass. The equation of the motion given by Equation (19) can be simplified by expressing $\theta_L(t)$ and $\tau_L(t)$ in terms of $\theta_m(t)$ and $\tau_l(t)$.

$$\tau_L(t) = \frac{r^2 J_L}{\eta}\ddot{\theta}_m(t) + \frac{r}{\eta}\tau_g(t) \tag{20}$$

where $\tau_g(t)$ is the gravitational torque and if J_{eff} is the effective moment of inertia. Equation (20) is combined with equation (10) in the simplified motor equation.

$$\frac{k_m}{R_m}u_m(t) = J_{eff}\ddot{\theta}_m(t) + B\dot{\theta}_m(t) + \frac{r}{\eta}\tau_g(t) \tag{21}$$

$$\tau_g(t) = mgl_c cos\theta_L(t) \tag{22}$$

Equation (22) indicates that the gravitational torque component exists even when the motor is kept in any direction without load conditions because $m = m_s + m_L$. But for correct functionality, $\tau_g(t)$ must be compensated. This can be achieved based on the direct torque control technique. Let $\dot{\theta}_m(t'_0)$ and $\theta_m(t'_0)$ represent the initial conditions for angular position and velocity of a motor, respectively. An external force $F_e(t)$ is created from a direct tactile sensation to the end of the robot during a time interval $[t_0, t_f]$, and no force is applied when $t > t'_f$. The end-effector moves to $\theta_m(t'_f)$ during the interval when the external force Fe(t) is applied, and its velocity is $\dot{\theta}_m(t'_f)$. The objective of gravity torque control is to develop a controller that meets the requirement that the robot can stop in any position when no external force is applied. When there is no external force, the condition to be met is that the velocity must be zero . If θ_{md} is the desired angular velocity, then:

$$\theta_{md} = 0, t > t'_f \tag{23}$$

From equation (21)

$$u(t) = J_{eff}v(t) + B\dot{\theta}_m(t) + \frac{r}{\eta}\tau_g(\theta_m(t)) \tag{24}$$

Where $u(t) = \frac{K_t}{R_m}u_m(t)$, the motor's input voltage is $u_m(t)$, and v(t) represents an input signal. With the goal of using viscous damping as a break, which reduces velocity to near zero and hence makes the $B\theta_m(t)$ term can be estimated [11] and essentially negligible. Therefore, assuming perfect cancellation of the gravity torque, the system can be linearized with the following equation for $t > t'_f$.

$$v(t) = \ddot{\theta}_m(t) + \frac{B}{J_{eff}}\dot{\theta}_m(t) \tag{25}$$

If K_D is the design constant, then

$$v(t) = \frac{K_D}{J_{eff}}\dot{\theta}_m(t) \tag{26}$$

So

$$u(t) = -K_D\dot{\theta}_m(t) + \frac{r}{\eta}\tau_g(\theta_m(t)) \tag{27}$$

C. Disturbance Observer modelling

Equation (3) consists of a couple of parameters motor inertia and torque constant, which can be changed because of several properties. Similarly, due to the mechanical configuration of the motion system, the inertia might also change. In the case of the torque coefficient, it changes with respect to the rotor position of the electric motor, which causes the irregularity in the distribution of the magnetic flux throughout the surface of the rotor [6, 2]

$$J_m = J_n + \Delta J \tag{28}$$

$$K_t = K_{tn} + \Delta K_t \tag{29}$$

Where;
J_n : Nominal inertia
ΔJ : Inertia variation
K_{tn} : Nominal torque coefficient
ΔK_t : Variation of torque coefficient

By substituting equations (28) and (29) into equation (3), equation ((30) obtained:

$$(J_n + \Delta J)\ddot{\theta}_m = (K_{tn} + \Delta K_t){i_a}^{ref} - \tau_l \tag{30}$$

By rearranging,

$$J_n\ddot{\theta}_m = K_{tn}{i_a}^{ref} - (\tau_l + \Delta J\ddot{\theta}_m - \Delta K_t{i_a}^{ref}) \tag{31}$$

From equations (28) and (29) Disturbance Torque (τ_{dis})

$$\tau_{dis} = \tau_{int} + \tau_{ext} + B_m\dot{\theta}_m(t) + \Delta J\ddot{\theta}_m - \Delta K_t{i_a}^{ref} \tag{32}$$

Apparently, the disturbance torque comprises all the internal torques, external torques, friction torques and torques due to parameter variations and all of them compensated so that the accurate output torque obtained. From equation (31) τ_{dis} can be calculated as follows.

$$\tau_{dis} = K_t{i_a}^{ref} - J_n\ddot{\theta}_m \tag{33}$$

Using the known values at the right-hand side, the unknown value of τ_{dis} can be determined using the known values at right-hand side in the above equation. Using the velocity response $\dot{\theta}$ and the torque current ${i_a}^{ref}$, the estimated disturbance torque $\hat{\tau}_{dis}$ is obtained. As shown in equation (34), the estimation is done through a first-order low-pass filter, where g_{dis} represents the cut-off frequency of the low-pass filter.

$$\hat{\tau}_{dis} = \frac{g_{dis}}{s + g_{dis}}\tau_{dis} \tag{34}$$

The significance of the disturbance detected in practical application is observed as disturbance compensation as well as in the reaction torque estimation [14]. The external torque acting on the slave manipulator is considered as the Reaction torque and from equation (32) it is calculated as:

$$\tau_{ext} = \tau_{dis} - [\tau_{int} + B_m\dot{\theta}_m(t) + \Delta J\ddot{\theta}_m - \Delta K_t{i_a}^{ref}] \tag{35}$$

Since at the moment of contact,

$$\tau_{ext} = \tau_{react} \tag{36}$$

Where :
τ_{react} : Reaction Torque

$$\tau_{react} = \tau_{dis} - [\tau_{int} + B_m\dot{\theta}_m(t) + \Delta J\ddot{\theta}_m - \Delta K_t{i_a}^{ref}] \tag{37}$$

The disturbance observer offers numerous advantages including observation of disturbance torque and compensation. While a regular force sensor consists of narrow bandwidth, the disturbance observer offers relatively wider bandwidth [1].

III. RESULTS AND DISCUSSION

As mentioned in the system modeling a system is modeled in MATLAB R2020b (Simulink) and respective graphs (Fig 3 to Fig 8) of outputs are observed. The experimental parameters used in the Simulink are given in Table I and the considered actuator parameters are given in Table II. System parameters such as motor torque, inertia, nominal inertia, nominal motor torque, low pass filter coefficients, and so on are adjusted as a result of the modeling.

TABLE I
THE EXPERIMENTAL PARAMETERS

Parameter	Symbol	Values	Units
Motor Inertia	J_n	0.2	$Kgcm^2$
Torque Coefficient	K_t	24	Ncm/Amp
Proportional Constant(Master)	K_p	-1.7518366	rad/sec
Derivative Constant(Master)	K_d	-12.861871	Rad/sec
Proportional Constant(Slave)	K_p	3026.43536	rad/sec
Derivative Constant(Slave)	K_d	160.230491	Rad/sec

TABLE II
DC MOTOR SPECIFICATIONS

Specification of motors	
Rated output	0.1 kW
Rated/max torque	25.3 Nm
Encoder resolution	1003846 Pulse/rev

From the previous work on the author's moment of inertia, torque coefficient, and frictional components, it can be compensated for these parameters [11]. So by substituting the accurate values for the parameters the RTOB output should be obtained as zero after friction compensation. The DOB output must be the same as the provided disturbance since it is used to estimate the value of the disturbances. After getting these outputs it is concluded that the RTOB and DOB are efficiently functioning in both contexts, estimation, and compensation. Now while comparing the position of both master and slave the values of both should be similar, because only then the slave system will follow the same trajectory as that of the master system.

By substituting various values of cut-off frequency, the best results should be obtained out of the system. Through the trial and error method, the RTOB output is measured as zero.

This means that while executing this as a real-time output, the obtained values other than zero in the result are completely the gravity and interactive torque (τ_δ). Therefore, the gravity torque and the interactive torque can be estimated accurately. Each of the disturbances is interpreted in detail in respective sections.

1) Without friction compensation
2) With friction Compensation

Considering the factor of friction in the given system, the compensated friction parameters will give a more accurate RTOB result. Here in the friction compensation both dynamic friction parameter and static friction parameter are considered. The circumstances that apply the same here in the system model are inferred from the estimation of friction parameters through mathematical computations. The results given below are a fine-tuned version of the above by introducing the friction compensation too.

For experimental purposes, external disturbances are given to the master and slave sides. Disturbances are applied at the motor of the master and slave respectively. The system is subjected to three sorts of disturbances which are Periodic, Supporting, and Opposing. Periodic disturbance considered here is a constant sinusoidal disturbance. Supporting provides torque in the direction of motion i.e. the disturbance is supportive in nature. Opposing disturbance acts in the opposite direction of motion and therefore, it is resistive in nature. Comparing the results with various disturbances applied, more accurate results can be obtained.

By comparing both 30 Hz and 1000 Hz reaction torque output as in Fig 3, Fig 5, and Fig 7, it is clearly visible that a higher cut-off frequency provides more accurate results. As a result of various other trials, it may be stated that 1000 Hz provides the most accurate outcome. Fig 4, Fig 6, and Fig 8 show the DOB Output Comparison of the system model for Master and Slave with cut-off frequency, Gdis 1000 Hz with Friction Compensation.

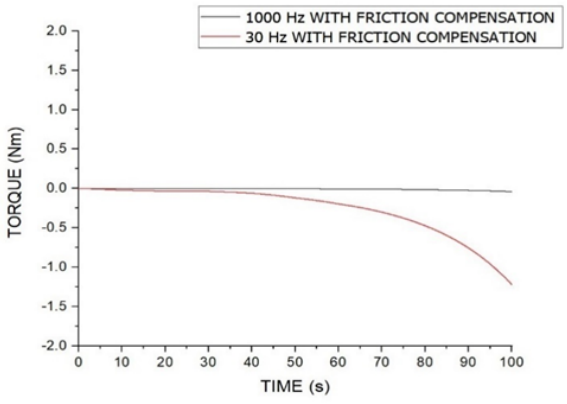

Fig. 3. Reaction Torque Output Comparison of system model with cut-off frequency, Gdis 30 Hz & 1000 Hz with Friction Compensation

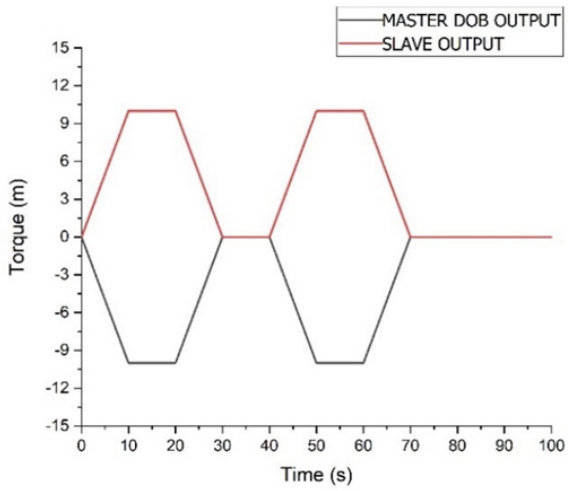

Fig. 4. DOB Output Comparison of system model for Master and Slave with cut-off frequency, Gdis 1000 Hz with Friction Compensation

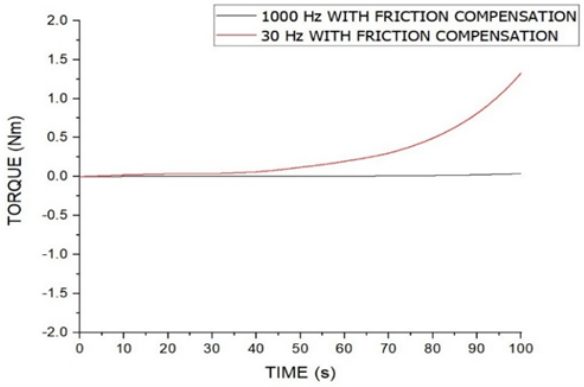

Fig. 5. Reaction Torque Output Comparison of system model with cut-off frequency, Gdis 30 Hz & 1000 Hz with Friction Compensation

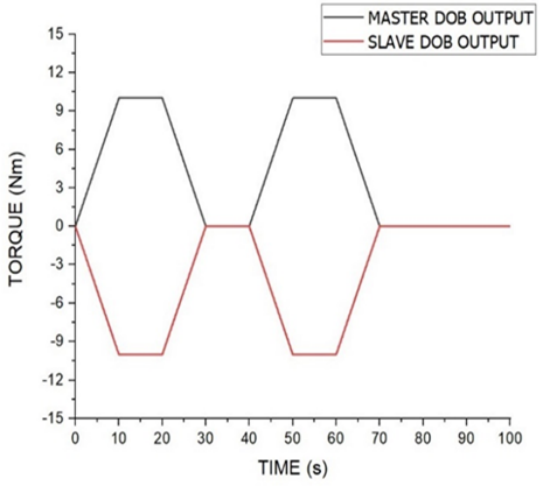

Fig. 6. DOB Output Comparison of system model for Master and Slave with cut-off frequency, Gdis 1000 Hz with Friction Compensation

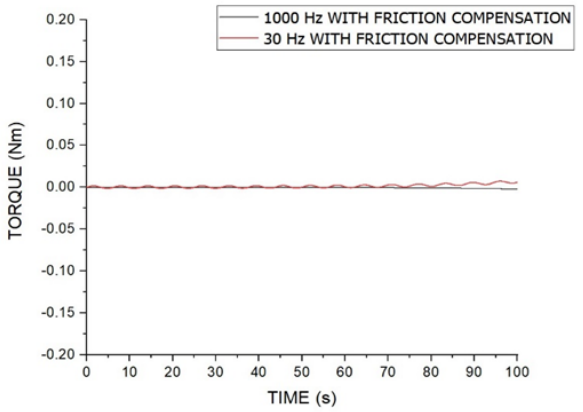

Fig. 7. Reaction Torque Output Comparison of system model with cut-off frequency, Gdis 30 Hz with Friction Compensation and Without Friction Compensation

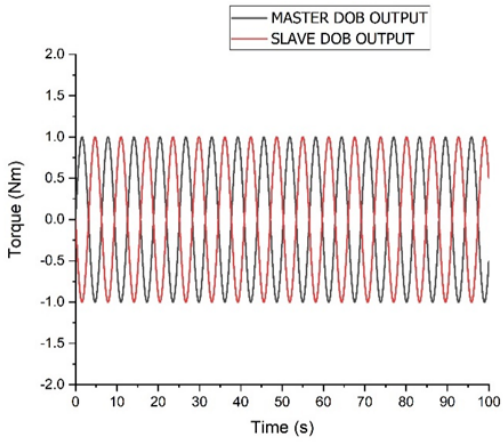

Fig. 8. DOB Output Comparison of system model for Master and Slave with cut-off frequency, Gdis 1000 Hz with Friction Compensation

IV. CONCLUSION

In this research, we proposed a new gravity torque estimation and compensating method for small DC motors. Sensorless torque sensors are employed throughout this study, with DOB serving as the disturbance torque sensor and RTOB serving as the external torque sensor. The DOB-based constant velocity test is used to determine the friction components. The calculated system parameters are used to perform friction compensation tests, which are then tested using the typical bilateral control system. The proposed approach for calculating the motor gravity torque yields more accurate results. MATLAB SIMULINK was used to verify the accuracy of the suggested friction compensation approach as well as the effect of parameters. The tests were conducted under the assumption that the system is linear.

REFERENCES

[1] AM Harsha S Abeykoon and Kouhei Ohnishi. "Improvement of tactile sensation of a bilateral forceps robot by a switching virtual model". In: *Advanced Robotics* 22.8 (2008), pp. 789–806.

[2] AM Harsha S Abeykoon and Hasala R Senevirathne. "Disturbance observer based current controller for a brushed DC motor". In: *2012 IEEE 6th International Conference on Information and Automation for Sustainability*. IEEE. 2012, pp. 47–52.

[3] Sari Abdo Ali et al. "The effect of parameters variation on bilateral controller". In: *International Journal of Power Electronics and Drive Systems* 9.2 (2018), p. 648.

[4] Carlos Canudas, K Astrom, and Konrad Braun. "Adaptive friction compensation in DC-motor drives". In: *IEEE Journal on Robotics and Automation* 3.6 (1987), pp. 681–685.

[5] Gopal K Dubey. *Fundamentals of electrical drives*. CRC press, 2002.

[6] Shigeyuki Funabiki and T Fukushima. "Current commands for high-efficiency torque control of DC shunt motor". In: *IEE Proceedings B (Electric Power Applications)*. Vol. 138. 5. IET. 1991, pp. 227–232.

[7] Hideyuki Kobayashi, Seiichiro Katsura, and Kouhei Ohnishi. "An analysis of parameter variations of disturbance observer for motion control". In: *IEEE Transactions on Industrial Electronics* 54.6 (2007), pp. 3413–3421.

[8] Hongbing Li et al. "Achieving haptic perception in forceps' manipulator using pneumatic artificial muscle". In: *IEEE/ASME Transactions on Mechatronics* 18.1 (2011), pp. 74–85.

[9] Ryo Minaki, Hiroshi Hoshino, and Yoichi Hori. "Driver steering sensitivity design using road reaction torque observer and viscous friction compensation to Active front steering". In: *2010 IEEE International Symposium on Industrial Electronics*. IEEE. 2010, pp. 155–160.

[10] Yuzuru Ohba et al. "Sensorless force control for injection molding machine using reaction torque observer considering torsion phenomenon". In: *IEEE Transactions on Industrial Electronics* 56.8 (2009), pp. 2955–2960.

[11] Branesh M Pillai and Jackrit Suthakorn. "Motion control applications: observer based DC motor parameters estimation for novices". In: *Int. J. Power Electron. Drive Syst* 10.1 (2019), pp. 195–210.

[12] Branesh M Pillai, Chumpon Wilasrusmee, and Jackrit Suthakorn. "Observer based dynamic control model for bilaterally controlled MU-lapa robot: Surgical tool force limiting". In: *International Journal of Electrical and Computer Engineering* 10.1 (2020), p. 828.

[13] Jianyong Yao, Zongxia Jiao, and Dawei Ma. "Adaptive robust control of DC motors with extended state observer". In: *IEEE transactions on industrial electronics* 61.7 (2013), pp. 3630–3637.

[14] Sung Min Yoon et al. "Bilateral control for haptic laparoscopic surgery robot". In: *IEEE ISR 2013*. IEEE. 2013, pp. 1–5.